Nitrogen doped carbon dots embedded in poly(ionic liquid) as high efficient metal-free electrocatalyst for oxygen reduction reaction

Thuan-Nguyen Pham-Truong, Christine Ranjan, Hyacinthe Randriamahazaka, Jalal Ghilane

Nitrogen doped carbon dots embedded in poly(ionic liquid) as high efficient metal-free electrocatalyst for oxygen reduction reaction

Thuan-Nguyen Pham-Truong, Christine Ranjan, Hyacinthe Randriamahazaka and Jalal Ghilane*

SIELE group, ITODYS Lab. – UMR 7086 CNRS, Chemistry Department, Université Paris Diderot, Sorbonne Paris Cité, 15 rue Jean Antoine de Baïf, 75013 Paris, France.

*Corresponding authors:

E-mail address: jalal.ghilane@univ-paris-diderot.fr

Abstract

Seeking for highly efficient and cost-effective catalysts towards electrochemical activation of small molecules is the key process in the development of renewable technologies. In this work the ionic liquid has been proposed as a promising candidate for elaborating of hybrid materials for multi-purposes in the fields of electrocatalysis. Precisely, the polymer brushes based ionic liquid, poly(imidazolium), were used as a platform for host guesting carbon-dots material and their electrocatalytic activity towards the oxygen reduction reaction was evaluated. The obtained results demonstrate that the presence of the poly(IL) shifts the ORR performance over carbon dots from 2 electron pathway, with hydrogen peroxide as the main product, to nearly 4 electron pathway. Thus, a switch from hydrogen peroxide generation (> 80%) to water production is obtained in the presence of the poly(IL) layer over a broad potential range. This synergetic effect is correlated to the chemical structure and the morphology of the immobilized polymer ionic liquid. Finally, the poly(IL) was demonstrated to be a powerful strategy for boosting the catalytic activity for a given carbon-dots catalyst towards efficient 4 electron ORR.

Keywords: Polymer ionic liquid; Carbon dots; Electrocatalysis; Oxygen reduction reaction.

1. Introduction

Increasing demands for renewable energy have attracted numerous studies for the development of low cost and efficient technologies that can highly convert chemical energy storage into usable electricity [1]. Electrochemical energy conversion based on oxygen reduction reaction (ORR) received great interest in the development of fuel cell technology [2]. For getting the catalytic effect, a given material has to satisfy several criteria including the

occurrence of the oxygen reduction by 4-electron pathway at low over potential. The reaction pathway for ORR depends strongly on the crystallographic structure [3], type of materials [4] and the pH of the reaction medium [5-8]. Among the various families of catalysts, platinum and its alloys appear as highly efficient for catalyzing the oxygen reduction with low over potential [9-12]. However, the other main remaining problem for oxygen reduction is the absorption step of the reactant onto the catalyst surface. Indeed, not only the electrochemical activation energy is needed for the reduction process but also the release of the intermediates from the surface is important step to avoid the passivation of the active surface [13]. Recently, ionic liquids and its derivatives have been used as additive to improve the oxygen reduction [14,15]. In particular, the composite metal-ionic liquid (IL) leads to ORR performance close to the benchmark of platinum-based catalysts [16]. The ionic liquid was used in solid-liquid biphasic catalysis by introducing a thin layer of ionic liquid onto porous solid support which gives an enhancement in term of performance toward oxygen reduction. Pt-Ni nanoporous nanoparticle impregnated with ionic liquid, [MTBD][beti], displays a strong enhancement of the ORR activity. This result was explained by the specific interaction between the ionic liquid and the oxygen which favors its adsorption onto the metallic active surface. However, the main problem of this family of catalysts is related to the ionic liquid leakage into the surrounding solvent, putting in restriction the choice of the solvent based on the nature of the selected ionic liquid.

Carbon based catalysts including graphene, carbon nanotube and nanoporous carbons have been proposed as emergent materials for the activation of ORR [17-19]. However, most of these materials undergoes ORR via 2-electron pathway towards H_2O_2 production [20]. Several effort have been achieved for moving the catalytic activity of carbon based material to 4-electron pathway. Thus, doping the carbon materials by heteroatoms (e.g. N, F, P) or their combination with other metals (Fe, Pt, Co..) lead to promote the catalytic activity of ORR [21-23].

Recently, the synthesis of carbon dots in aqueous media and ionic liquid (IL) media, via microwave assisted method, generate IL doped–nanoparticles. The microwave (MW) assisted synthesis is referred to a solvothermal process that involves the use of solvent under moderate to high pressure and temperature to facilitate the interactions between reactants [24]. The generated materials have been reported as an efficient catalyst for the hydrogen peroxide production [25]. However, for switching the catalytic activity of carbon dots towards ORR

from 2 to 4 electron pathway, additional treatment including doping with heteroatoms or metal is required [21-23].

In this work we purpose to investigate the synergetic effect between polymers based ionic liquid and carbon dots as a catalyst. The approach is based on the use of the glassy carbon electrode surface functionalized with polymer ionic liquid (poly(1-methyl-3-vinylimidazolium bis(trifluoromethane)sulfonimide)), Poly(VImM), using surface-initiated atom transfer radical polymerization (SI-ATRP) [26,27]. Next, the poly(VImM) modified electrode was decorated with carbon dots and the catalytic performance of the generated materials towards ORR was investigated. In previous reports, our group demonstrated the formation of nanostructured polymer brushes-like structure through the SI-ATRP process [27]. More interestingly, the generated polymer, poly(IL), showed a promising electrocatalytic activity for ORR that was linked to the chemical composition and the nanostructuration of the polymer [27]. Our approach is to design an efficient electrocatalyst by decorating the polymer brushes with N-doped carbon dots for oxygen reduction. This work paves the way for improving the catalytic performance of the ionic liquid based materials and for exploring the synergetic effect between poly(ionic liquid) and other materials towards metal-free catalyst.

2. Experimental section

2.1 Chemicals.

D-glucose (> 99%), L-Glutamine (>99%), 1-ethyl-3methylimidazolium ethylsulfate (EMIES) (> 95%), potassium hydroxide (> 99%), vinylimidazole (> 98%) and lithium bis(trifluoromethane)sulfonimide (> 99%) were purchased from Sigma Aldrich, methyliodide (> 99%) was obtained from Alfar Aesar. All the chemicals were used as received without any further treatments.

2.2 Synthesis of C-dots.

For this study, two C-dots were synthesized and labelled, C-dots(aq) generated from an aqueous solution containing glucose and glutamine, and C-dots(IL) generated from mixtures of glucose and ionic liquid (EMIES). The syntheses of C-dots(aq) were carried out in a microwave reactor (Anton Paar 300). Typically, 1.4 g of glucose and 0.7 g of glutamine were dissolved under vigorous stirring in 20 ml of distilled water resulting to clear transparent solution. Then the mixture was poured into a special-purpose vial for heating via microwave irradiation. The temperature ramp was constantly kept at $10°C.min^{-1}$. After 5 min of heating, the solution was cooled down to room temperature followed by dialysis using cellulose membrane (Spectra/Por® Dialysis Tubing with MWCO = 7 kDa) for 48 hrs. Finally, the

dialyzed suspensions of C-dots were centrifugated at 8000 rpm for 20 minutes to eliminate non-desired agglomerations and the supernatants were collected resulting to yellowish solutions and were ready for further uses.

The C–dots(IL) were synthetized as described in our previously reported study [25]. Accordingly, 1.4 g of glucose was dissolved in 20 ml of EMIES ionic liquid. Then, the solutions were heated with the microwave assisted method for 5 minutes at controlled temperatures with a temperature ramp at $10°C.min^{-1}$. Once the solutions were cooled down to room temperature, the C-dots solutions were purified by dialysis (MWCO = 7 kDa) followed by centrifugation at 8000 rpm for 20 minutes.

2.3 Preparation of Poly(VImM) and Poly(VImM)/C-dots

The preparation of surface functionalized with polymeric ionic liquid using surface-initiated atom transfer radical polymerization (SI-ATRP) was performed as previously reported [26-28]. Briefly, the initiator was attached electrochemically into electrode surface via electrochemical oxidation of 2-bromoethylamine using cyclic voltammetry. Later, the polymerization process was performed by dipping the initiated electrode into acetonitrile solution containing 3 mM of 1-methyl-3vinylimidazoliumTFSI, 4 µM of CuCl as catalyst, 2.8 µM of $CuCl_2$ and 5 µL of N,N,N′,N″,N″-Pentamethyldiethylenetriamine (PMDETA) as complexing agent under Argon flux. The reaction was maintained at 50°C for 2 hrs under inert atmosphere. Then the modified electrode was removed from the reaction medium, washed thoroughly with acetonitrile, acetone, and was sonicated in distilled water for 5 minutes. The C-dots were added to the poly(VImM) modified electrode by drop casting a solution containing the C-dots in a mixture H_2O/Methanol. Next, the poly(VImM)/C-dots electrode is dried at 70°C and then rinsed with water.

2.4 Instrumentations

For electrochemical measurements, a rotating ring disk setup was used. A saturated calomel electrode and a stainless steel mesh were used as reference electrode and counter electrode, respectively. A rotating ring disk electrode (E7R9 series) from Pine Research Instruments was used for the electrochemical measurements. XPS measurements of the modified electrodes were performed using a Thermo VG Scientific ESCALAB 250 system fitted with a microfocused, monochromatic Al Kα ($h\nu$ = 1486.6 eV) 200 W X-ray source. Zeta potential measurements were done using a Zetasizer Nano ZS (Malvern Instruments Inc.). Three size measurements and four zeta measurements were performed.

The particles size distribution of the as-prepared carbon dots were obtained via TEM image using a JEOL JEM 100CX.

For catalytic performance evaluations, a E7R9 ThinGap Fixed-Disk RRDE tips with 320 μm gap ($A_{GC\ disk}$ = 0.247 cm^2, $A_{Pt\ ring}$ = 0.187 cm^2) was used as working electrode, a carbon graphite rod (from Goodfellow) and saturated calomel electrode were used as counter electrode and reference electrode, respectively. In all experiments, the potential was converted to Reversible Hydrogen Electrode (RHE) via the following equation:

E (vs RHE) = E (vs SCE) + 0.241 + 0.059 pH

The electrochemical measurements were carried using a CHI920C bipotentiostat (CH Instruments, Austin, Texas). For oxygen reduction reaction measurements, 0.1 M KOH solution was used as electrolyte and bubbled with purified oxygen gas for 30 minutes. During the measurements, the solution was kept under O_2 atmosphere.

3. Results and discussion

3.1 Material characterization

The synthesis of carbon dots (CDs) in ionic liquid or in aqueous media leads to generate N-doped CDs with different ratio of graphitic and pyridinic nitrogen [25]. The CDs were drop casted onto poly(IL) brushes-like structure leading to poly(IL)/CDs hybrid material as a sketched in Fig 1.a. The chemical composition of N-doped CDs and poly(IL)/CDs were investigated by X-ray photoelectron spectroscopy (XPS).

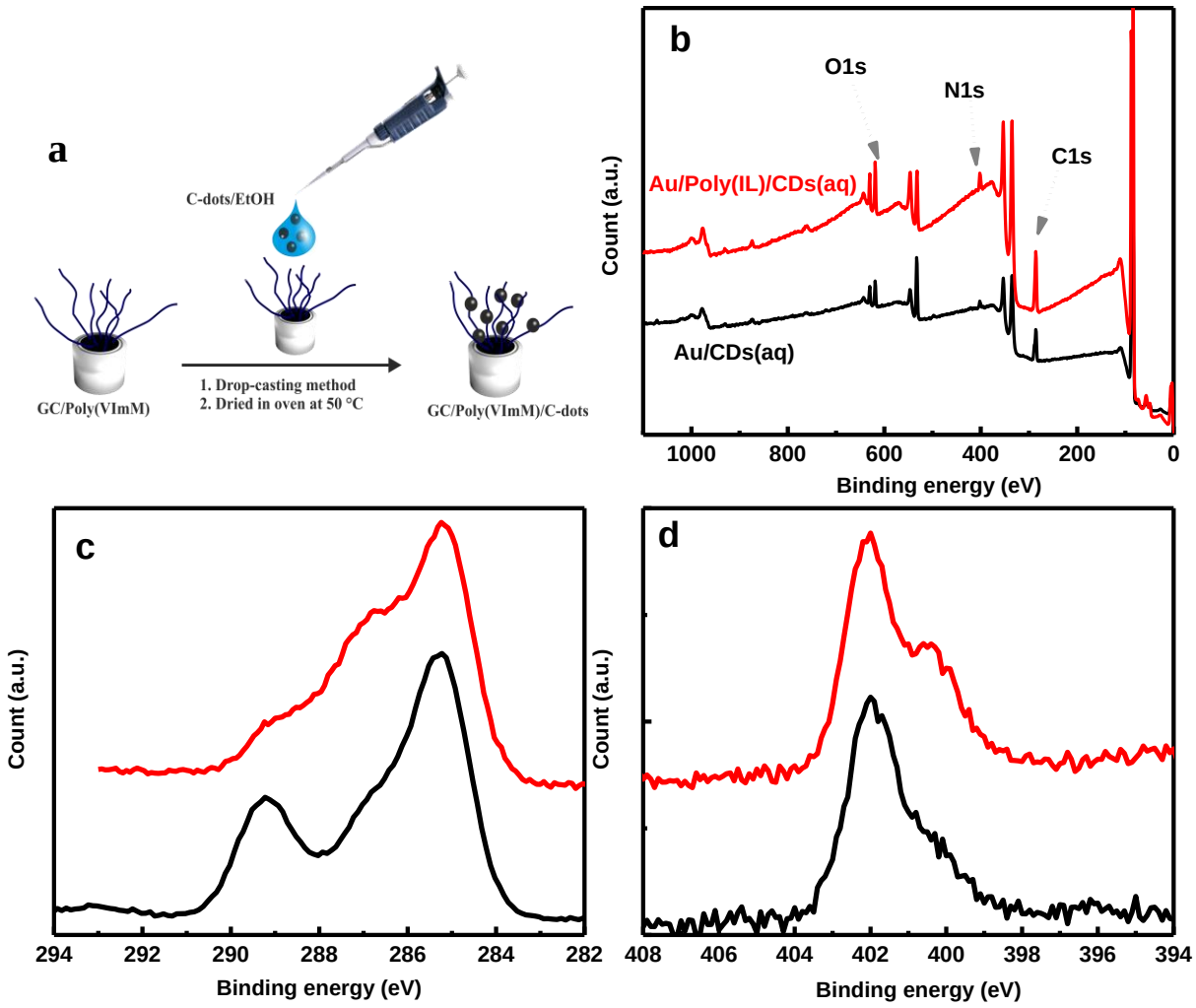

Fig. 1. *(a)* Scheme illustrating the deposition of CDs onto electrode surface. XPS spectra of CD(aq) (black curves) and Poly(VImM)/ CD(aq) (red curves): *(b)* Survey spectrum, *(c)* and *(d)* the corresponding high resolution XPS spectra of C1s and N1s, respectively.

Fig. 1b compares the XPS survey spectrum of CD(aq) drop casted onto Au substrate (black curve) and onto Au/poly(IL) (red curve). This comparison displays the contribution of three main components C1s, N1s and O1s with different atomic ratio. The deconvolution of the C(1s) spectrum of Au/CD(aq), Fig. 1c (black curve), shows the presence of 3 components. These signals correspond to C-C/C-H_x (285.42eV), C-O (287 eV), C-N (286 eV) and COO (289.3 eV). Besides that, the C1s recorded on Au/poly(IL)/CD(aq) shows additional peak located at 286.5 eV attributed to N-C-N band. Next, the N1s spectrum, Fig. 1d, shows the presence of two main contribution related to different nitrogen bonding states. These peaks are attributed to the pyridinic-like and graphitic nitrogen at binding energy 400 eV and 401.8 eV, respectively. In the case of Au/CD(aq) the graphitic-like nitrogen represents the predominant form, while for the Au/poly(IL)/CD(aq) the contribution of the pyridinc-N increase. Thus, for the CD(aq) the total atomic percentage of N is around 5% which is a

contribution of 4% of graphitic like nitrogen and 1% of pyridinic nitrogen form. In the case of poly(IL)/CD(aq) sample, the atomic percentage of nitrogen is higher and reach 8% due to the contribution of imidazolium polymer. The total amount of nitrogen is a contribution of graphitic like nitrogen at 5% and an amount of 3% of pyridinic nitrogen. Similar results and nitrogen distribution were observed in the case of the CDs generated in ionic liquid, CDs(IL) [25]. Overall, the XPS investigations confirm the formation of N-doped carbon dots and the presence of graphitic and pyridinic nitrogen.

The size distribution of CDs(aq) and CDs(IL) were characterized using Dynamic Light Scattering and TEM image. As shown in the Fig. 2a, the hydrodynamic diameter of the carbon dots remains similar for both types of particles (~ 100 nm).

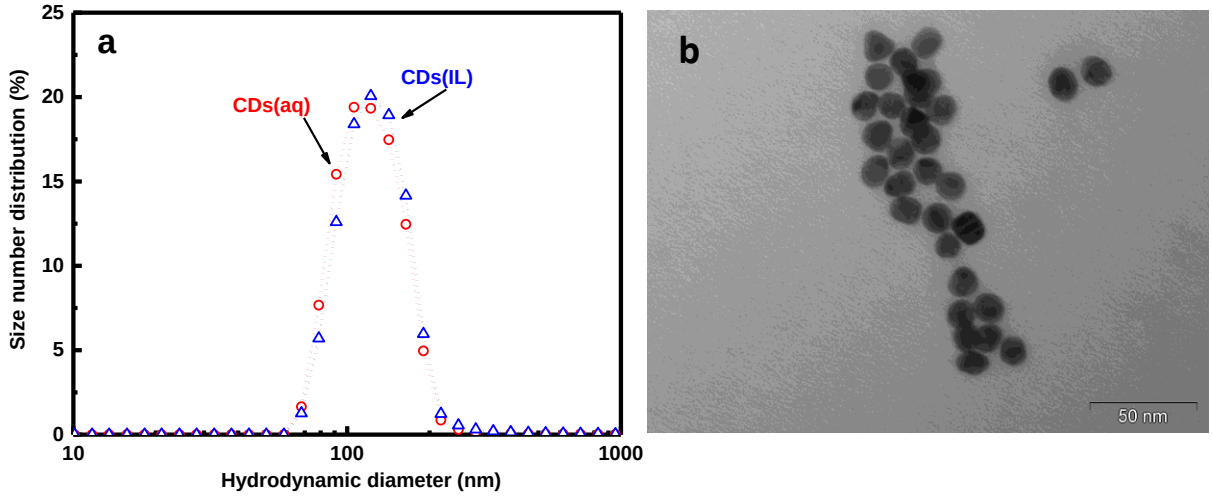

Fig. 2. (a) Size distribution measured by DLS for CD(aq) (red) and CD(IL) (blue); (b) TEM image of CD(aq).

However, TEM image (Fig. 2b) shows fairly uniform carbon dots with a diameter around 7-16 nm (11.5 nm in average). Even though the carbon dots do not swell in water, aggregation can be observed which explain the obtained difference in term of size distribution measured in solution (DLS) and at the surface (TEM). Additional information about the surface charge of the C-dots can be determined by using Zeta potential measurements affording a value of – 24 ± 5 mV and -25 ± 6 mV for CDs(aq) and CDs(IL), respectively.

3.2 Catalytic activity of N-doped Carbon dots

The catalytic activity of the CDs(aq) towards the oxygen reduction reaction was investigated using rotating ring disk electrode (RRDE) in alkaline solution. Fig. 3a displays the variation of ring and disk current as function of the potential at different rotation speed.

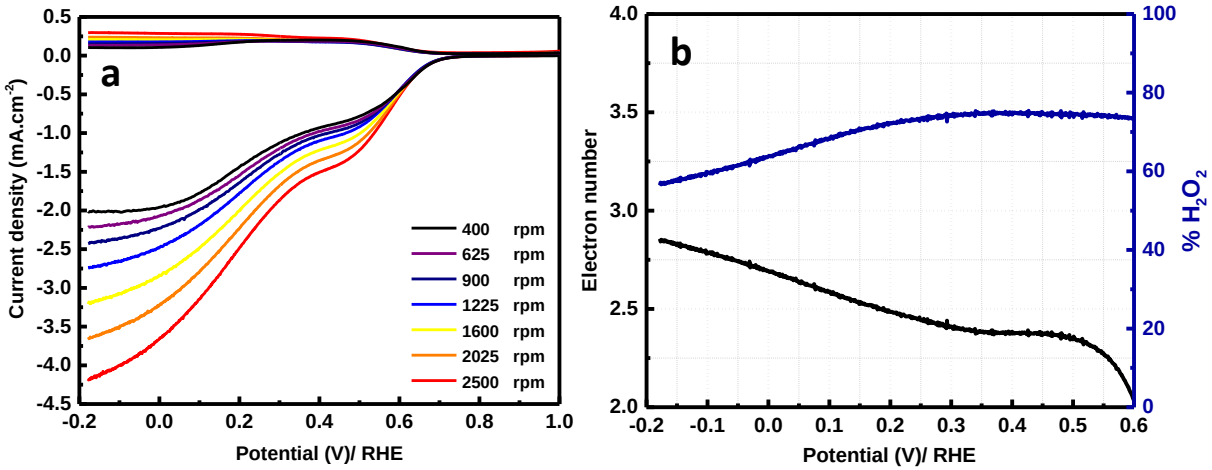

Fig. 3. (a) ORR polarization curves using RRDE (ring and disk current) at different rotations speeds for GC/CD(aq) in O_2-saturated 0.1 M KOH solution ***(b)*** Evolution of the electron number (black curve) and $\%H_2O_2$ (blue curve) as function of the potential of GC/CD(aq).

The disk current represents the electrochemical oxygen reduction, while the ring current collects the oxidation current of the generated hydrogen peroxide at the disk electrode. All the recorded LSV curves display a first reduction wave at 0.6 V followed be a second reduction at -0.2 V. The typical two-step reduction suggests the preferential ORR at CDs(aq) via a successive two-electron reaction pathway. Fig. 3b shows the evolution of the transferred electron number and the efficiency of hydrogen peroxide production as function of the potential. The electron number is around 2.2 for a potential ranged from 0.6 to 0.3 V and for more reducing potential the electron number increase and reach 2.7 at -0.2 V. This variation is consistent with the hydrogen peroxide evolution, confirming that the ORR on CDs(aq) catalyst is mainly governed by 2 electron process with a high production of hydrogen peroxide ranged from 75 to 55%. Overall, these results suggest that the first reduction step is attributed to the 2 electron reduction of oxygen leading to the formation of H_2O_2. Next, for more positive potential the electron number increases with a decrease in the H_2O_2 formation.

3.3 *Catalytic activity of N-doped CDs(aq)/Poly(VImM)*

To evaluate the electrocatalytic performance of our materials, the N-doped CDs were deposited onto poly(VImM) modified glassy carbon electrodes. Fig. 4a displays the LSVs curves recorded as function of the rotation speed, from 400 to 2500 rpm, at scan rate 10 $mV.s^{-1}$.

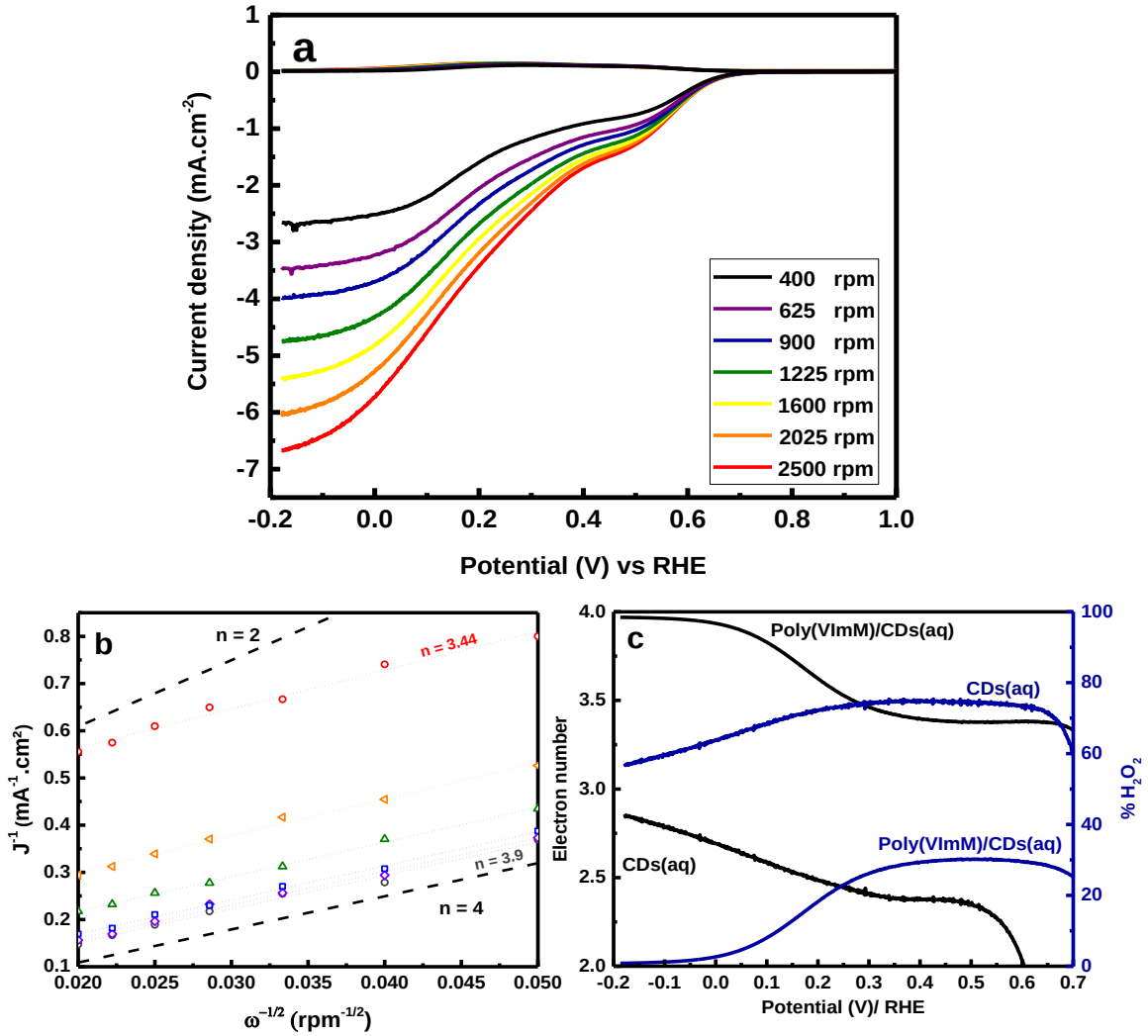

Fig. 4. (a) ORR polarization curves using RRDE at different rotations speeds for GC/poly(VImM)/CDs(aq) in O_2-saturated 0.1 M KOH solution; ***(b)*** Koutecky-Levich plot for GC/poly(VImM)/CDs(aq) at different potential. ***(c)*** Evolution of the electron number (black curves) and $\%H_2O_2$ (blue curves) as function of the potential recorded on GC/poly(VImM)/CDs(aq) and GC/CDs(aq).

In this case, two reduction waves were observed with all the studied materials. However, when compared to Fig. 3a the current density for poly(VImM)/CDs(aq) electrode is higher suggesting a better catalytic activity of the hybrid material. To get further insight, the variation of the current density as function of the rotation speed as well the electron number and the hydrogen peroxide production variation with the potential were recorded (Fig. 4b and c).

Interestingly, by adding C-Dots(aq) to the modified GC, the calculated electron transfer number using the Koutecky-Levich (K-L) plots, was found to be at n_e = 3.5 at 0.6 V vs. RHE which was strongly enhanced compared with the electron number provided by each component. In addition, from 0 to -0.2 V vs. RHE, the electron number reaches saturation

level close to 4 electrons (n_e = 3.9). The results are evidenced by calculating the n_e and the quantity of hydrogen peroxide as shown in Fig. 4c. The quantity of hydrogen peroxide decreases and reaches a lowest value around 3 % at -0.2 V vs. RHE. This result indicates the high selectivity for ORR activity of the prepared material by forming water as a final product.

The observed change of the catalytic reduction of ORR, of CDs after deposition onto poly(VImM) is certainly related to the synergetic effect between the Poly(IL) and CDs. The combination poly(IL) and CDs(aq) may generate and expose a new catalytic site more favorable for the ORR following the $4e^-$ pathway. The enhancement of the ORR performance of the hybrid material might correspond to a strong interaction between the positive charge provided by imidazolium ring and the N-doped C-Dots. According to the reported work about the interaction between ionic liquid (EMI^+SCN^-) and graphene surface, different interactions can be occurred at this interface [29]. The π-π stacking effect between the imidazolium aromatic ring and the conjugated C planes of the graphene can be one of the factors for the adhesion of the C-Dots onto poly(VImM). However, as the synthetized C-Dots contains partially amorphous structure, the present π-π stacking effect cannot be considered as the main interaction between the 2 components. The presence of electrostatic interaction could explain the synergetic effect. Indeed, the positive charge of imidazolium ring can attract the nitrogen and oxygen contained functional groups (the measured zeta potential of CD(aq) ζ-$E_{CDs(aq)}$ = -24 ± 5 mV). The electrostatic interaction involves the decrease of the electron density of not only the most acidic proton of imidazolium ring but also the nearby carbon active sites from the pyridinic nitrogen (N_P) of the C-Dots. This effect could favor the adsorption of oxygen and the reduction process should be easier. In the literature, several works investigated the active site for oxygen reduction reaction on N-doped carbon materials. It has been reported that the graphitic nitrogen is responsible for the electrochemical oxygen reduction and that the carbon atoms close to pyridinic nitrogen are the most active sites [30-33]. In addition, the acidic character of hydrogen in position 2, within the imidazolium, may act as a proton carrier and participate through the efficient O—O bond activation. Indeed, in the absence of this proton, replaced by methyl group, the electrocatalytic activity decreased highlighting the role of the acidic H within the imidazolium in the mechanism of ORR [27]. Overall, the mechanism of ORR onto CD's supported polymer based ionic liquid is still inconclusive, however, combining the experimental results and the works reported on N-doped carbon materials as electrocatalyst, the mechanism could be proposed as illustrated in Figure 5.

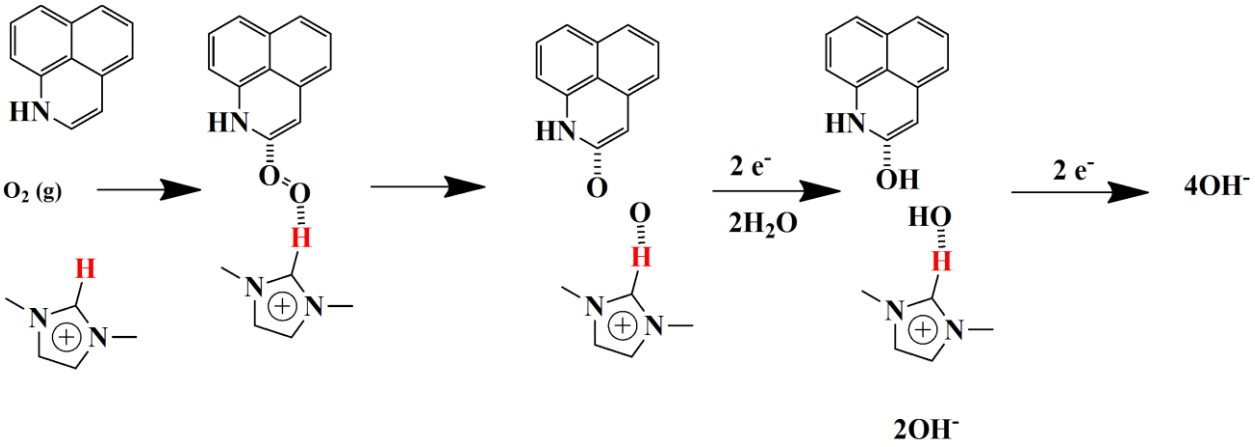

Fig. 5. Proposed mechanism for oxygen reduction using Poly(VImM)/CDs(aq).

The dissociative mechanism in the case of poly(VImM) is strongly unfavorable because of the high flexibility of the chains. By embedding the C-dots inside the film, the degree of freedom of the polymer brushes decreases leading to a less flexible system and higher ionic transport. The electrostatic interaction between the ionic liquid polymer and the N-doped C-dots generates new active sites in which the oxygen can interact with both components as shown in Fig.5. In addition, the size of the C-dots is around 10 nm corresponding to a surface area around 314 nm² with a high concentration of nitrogen functional groups. Resulting from the large surface of the C-dots, a large quantity of the ionic liquid-C active sites of C-dots can be formed leading to the formation of a high concentration of the dual active sites at the interface C-dots and poly(ionic liquid). This process can be associated to a dissociative mechanism, where the oxygen binds to the catalyst surface via two adjacent active sites under conditions where the distance between 2 active sites has to be equal to the length of the molecular oxygen bond. We suggest that the molecular oxygen migrates into the active site, one head is linked to the C(2) of imidazolium ring by hydrogen bonding while the other head is linked to the C(2') of the C dots which is adjacent to the nitrogen functional group. The O = O bond is broken with one oxygen atom at C dots surface and one oxygen atom adsorbed at ionic liquid chain.

In order to demonstrate clearly the important role of polymeric ionic liquid during the oxygen reduction reaction, the as-prepared CDs(IL) and poly(IL)/CDs(IL) were used as a catalyst. The latter was found to be an efficient for hydrogen peroxide production with a selectivity up to 95% for a potential ranged from 0.7 to 0.1 V. In term of current density, it is clearly displayed that in the first potential range, [0.7V; 0.3V], the current density provided by polymer/CDs(IL) hybrid is lower than the value obtained in the absence of the poly(IL) system (Fig. 6a).

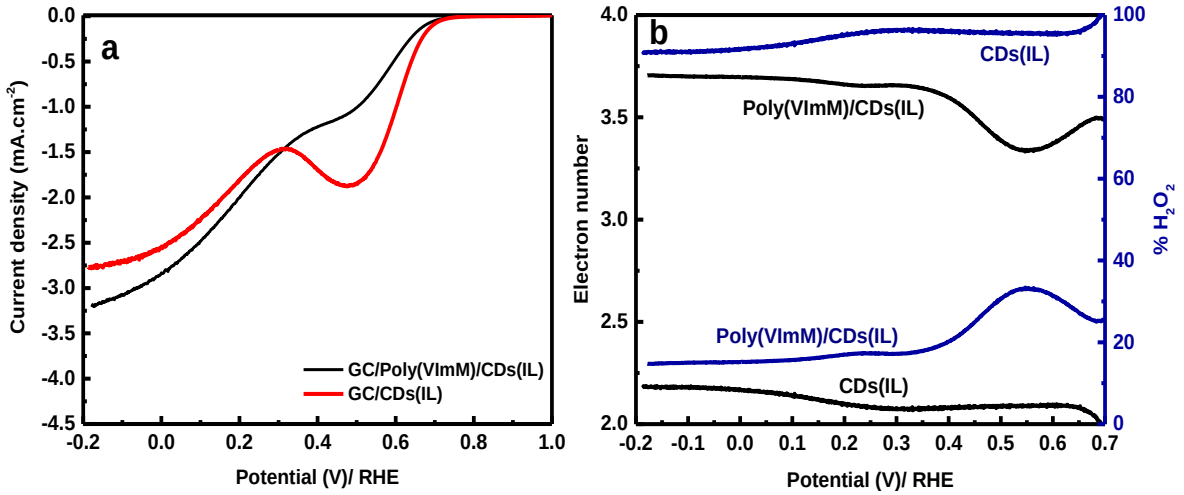

Fig. 6. (a) ORR polarization curves using RRDE. Red line for CDs(IL) deposited onto GC and black line for CDs(IL) deposited over the Poly(VImM)/GC. ***(b)*** Variation of the electron number (black curves) and $\%H_2O_2$ (blue curves) in function of the potential for GC/Poly(VImM)/CDs(IL) and GC/CDs(IL).

This result could indicate that the diffusion inside the catalytic film change in the presence of the polymeric film. The Poly(VImM) brushes create water channel to conduct oxygen molecules to the active sites [34]. In this configuration, the interaction between the imidazolium rings and the pyridinic nitrogen (within the CDs(IL)) could induce an oxygen orientation towards the duel active sites (C(2)–H ⋯ C/N_p) leading to a hindrance of the N_g catalytic sites [30]. However, in lower potential region, the current density of the substrate in the presence of polymer chains is higher when compared to the value offered by GC/CDs(IL), which is coherent with the proposed mechanism. The Fig. 6b shows that the number of exchanged electrons is strongly enhanced from 2 – 2.2 to 3.4 – 3.7 for two potential windows. Consequently, the percentage of hydrogen peroxide decreases from 90% down to 20% in the potential ranging from 0.2 to -0.2 V/ RHE using GC/Poly(VImM)/CDs(IL).

Fig. 7 summarizes the number of transferred electron and the quantity of hydrogen peroxide generated at -0.2 V/ RHE. For clear comparison, similar experiments were performed using poly(vinyl imidazole) brushes like structure.

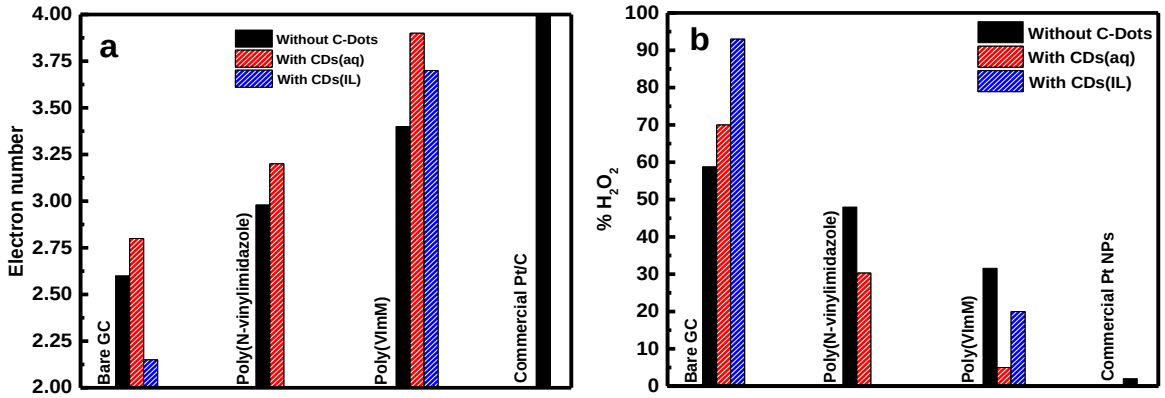

Fig. 7. Summary on the electrocatalytic performance in presence (red) and in absence (black) of C- dots: ***(a)*** electron number and *(b)* quantity of hydrogen peroxide at -0.2 V/ RHE.

Significantly, the poly(vinyl imidazole) shows a restraint affinity towards C-dots with similar number of electron and hydrogen peroxide rate in presence and in the absence of C-dots, confirming the crucial role of the cationic properties of the polymeric ionic liquid layer. Briefly, we have investigated a facile route for making efficient full organic electrocatalyst toward oxygen reduction reaction. The hybrid material poly(ionic liquid)/CDs(aq) exhibits a high selectivity for reducing oxygen to water (95 %) at -0.2 V vs RHE. Our preliminary results demonstrate that the interaction between ionic liquid and carbon-based materials is strongly involved into the oxygen reduction mechanism. In addition, our approach provides green materials with low cost means catalysts for further applications in metal-air batteries and fuel cell.

4. Conclusion

In conclusion, we have investigated a facile route for making efficient full organic electrocatalyst toward oxygen reduction reaction. The hybrid material poly(ionic liquid)/carbon dots exhibits high selectivity for reducing oxygen to water (97 %) at -0.2 V vs RHE. Our preliminary results demonstrate that the interaction between ionic liquid and carbon-based materials is strongly involved into the reduction mechanism. In addition, the polymer brushes structure could act as a platform for hosting various catalysts and more interestingly providing a synergetic effect that enhance the catalytic activity of the hybrid material towards ORR via $4e^-$ pathway. Our results show that this strategy is efficient even for catalyst with high selectivity to hydrogen peroxide (ORR through the $2e^-$ process). The proposed approach could either replace the need of catalyst doping or to some extent be combined to other non-noble-metal and doped carbon catalysts.

Acknowledgment

The authors acknowledge Dr. Philippe Decorse for XPS measurements. ANR (Agence Nationale de la Recherche) and CGI (Commissariat à l'Investissement d'Avenir) are gratefully acknowledged for their financial support of this work through Labex SEAM (Science and Engineering for Advanced Materials and devices) ANR 11-LABX-086, ANR 11-IDEX-0005-02.

References

[1] M. Shao, Q. Chang, J.P. Dodelet, R. Chenitz, Chem. Rev. 116 (2010) 3594–3657.
[2] L. Carrette, K.A. Friedrich, U. Stimming, Fuel Cells 1 (2001) 5–39.
[3] M. Kato, N. Oyaizu, K. Shimazu, I. Yagi, J. Phys. Chem. C. 120 (2016) 15814–15822.
[4] Y. Liu, W.E. Mustain, J. Am. Chem. Soc. 135 (2013) 530–533.
[5] C.-C. Chang, T.-C. Wen, H.-J. Tien, Electrochim. Acta. 42 (1997) 557–565.
[6] C.-C. Chang, T.-C. Wen, Mater. Chem. Phys. 47 (1997) 203–210.
[7] C.C. Hu, T.C. Wen, Electrochim. Acta. 41 (1996) 1505–1514.
[8] L. Yat-June, C.-C. Chang, T.-C. Wen, Ind. Eng. Chem. Res. (1996) 4767–4771.
[9] U.A. Paulus, T.J. Schmidt, H.A. Gasteiger, R.J. Behm, J. Electroanal. Chem. 495 (2001) 134–145.
[10] Y. Nie, L. Li, Z. Wei, Chem. Soc. Rev. 44 (2015) 2168–201.
[11] S.M. Alia, K.O. Jensen, B.S. Pivovar, Y. Yan, ACS Catal. 2 (2012) 858–863.
[12] A. Damjanovic, A. Dey, J.O. Bockris, Electrochim. Acta. 11 (1966) 791–814.
[13] D.B. Sepa, M. V Vojnovic, L.M. Vracar, A. Damjanovic, Electrochim. Acta. 32 (1987) 129–134.
[14] K. Ding, M. Zhao, Q. Wang, Russ. J. Electrochem. 43 (2007) 1082–1090.
[15] G.-R. Zhang, B.J.M. Etzold, J. Energy Chem. 25 (2016) 199–207.
[16] J. Snyder, T. Fujita, M.W. Chen, J. Erlebacher, Nat. Mater. 9 (2010) 904–7.
[17] L. Tao, Q. Wang, S. Dou, Z.L. Ma, J. Huo, S.Y. Wang, L.M. Dai, Chem. Com. 52 (2016) 2764–2767.
[18] K. Waki, R.A. Wong, H.S. Oktaviano, T. Fujio, T. Nagai, K. Kimoto, K. Yamada, Energy Environ. Sci. 7 (2014) 1950–1958.
[19] W. Wei, Y. Tao, W. Lv, F.Y. Su, L. Ke, J. Li, D.W. Wang, B. Li, F. Kang, Q.H. Yang, Sci. Rep. 4 (2014) 6289.
[20] H. Liu, Q. Zhao, J. Liu, X. Ma, Y. Rao, X. Shao, Z. Li, W. Wu, H. Ning, M. Wu, Appl. Surf. Sci. 432 (2017) 909–916.
[21] J.T. Zhang, Z.H. Zhao, Z.H. Xia, L.M. Dai, Nat. Nanotechnol. 10 (2015) 444–452.
[22] J.J. Duan, S. Chen, M. Jaroniec, S .Z. Qiao, ACS Catal. 5 (2015) 5207–5234.
[23] S. Rojas-Carbonell, C. Santoro, A. Serov, P. atanassov, Electrochem. Commun. 75 (2017) 38–42.
[24] S. Mao, Z. Wen, T. Huang, Y. Hou, J. Chen, Energy Environ. Sci. 7 (2014) 609–616.
[25] T.N. Pham-Truong, T. Petenzi, C. Ranjan, H. Randriamahazaka, J. Ghilane, Carbon 130 (2018) 544–552.
[26] V.B. Thi-Tuyet, G. Trippé-Allard, J. Ghilane, H. Randriamahazaka, ACS Appl. Mater. Interfaces 8 (2016) 28316–28324.
[27] T.N. Pham-Truong, H. Randriamahazaka, J. Ghilane, ACS Catal. 8 (2018) 869–875.
[28] T.N. Pham-Truong, H. Randriamahazaka, J. Ghilane, Electrochem. Commun. 82 (2017) 25–29.
[29] A.S. Pensado, F. Malberg, M.F.C. Gomes, A.A.H. Pádua, J. Fernández, B. Kirchner, RSC Adv. 4 (2014) 18017–18024.
[30] N. Wang, B. Lu, L. Li, W. Niu, Z. Tang, X. Kang, S. Chen, ACS Catal. 8 (2018) 6827–6836.
[31] T. Xing, Y. Zheng, L.H. Li, B.C.C. Cowie, D. Gunzelmann, S.Z. Qiao, S. Huang, Y. Chen, ACS Nano. 8 (2014) 6856–6862.
[32] Q. Lv, W. Si, J. He, L. Sun, C. Zhang, N. Wang, Z. Yang, X. Li, X. Wang, We. Deng, Y. Long, C. Huang, Y. Li, Nat. Commun. 9 (2018) 3376.
[33] X. Lu, D. Wang, L. Ge, L. Xiao, H. Zhang, L. Liu, J. Zhang, M. An, P. Yang, New J. Chem. 42 (2018) 19665–19670.
[34] G.R. Zhang, B.J.M. Etzold, Journal of Energy Chem. 25 (2016) 199–207.